# Sharp-interface imaging in full waveform inversion using finite elements

Keith J. Roberts (WS4), Antoine Laurain (WS1)
& Yuri F. Albuquerque (WS1)

Workstream 1: *Optimization of finite-difference seismic wave solvers and their adjoints*

Workstream 4: *Automatic generation and adaptation an unstructured meshes*

## Shell technical meeting - 18/05/2021

We gratefully acknowledge support of the RCGI - Research Centre for Gas Innovation, hosted by the University of São Paulo (USP) and sponsored by FAPESP - São Paulo Research Foundation (2014/50279-4) and Shell Brasil.

# Acoustic wave equation

- 2D acoustic wave equation with Perfectly Matched Layer (PML)

$$
\begin{aligned}
\partial_{tt}^2 u + \operatorname{tr}\Psi_1 \partial_t u + \operatorname{tr}\Psi_2 u - \nabla\cdot(c^2\nabla u) - \nabla\cdot \boldsymbol{p} &= c^2 f, \text{ in } \mathcal{D}\times[0,T]\\
\partial_t \boldsymbol{p} + \Psi_1 \boldsymbol{p} + \Psi_2(c^2\nabla u) &= 0 \text{ in } \mathcal{D}\times[0,T],\\
u\big|_{t=0} &= 0 \text{ in } \mathcal{D},\\
\partial_t u\big|_{t=0} &= 0 \text{ in } \mathcal{D},\\
\boldsymbol{p}\big|_{t=0} &= 0 \text{ in } \mathcal{D},\\
\partial_t u + c\nabla u\cdot \boldsymbol{n} &= 0 \text{ on } \Gamma\times[0,T]\\
\boldsymbol{p}\cdot\boldsymbol{n} &= 0 \text{ on } \Gamma\times[0,T]
\end{aligned}
$$

- $\mathcal{D}\subset\mathbb{R}^2$ is a rectangle with boundary $\Gamma$.
- $c$ is the P-wave velocity.
- $f$ is a source term.
- $\Psi_1, \Psi_2$ are damping matrices.

# Sharp-interface model

- $c$ is piecewise continuous: $c = c_0$ on $\Omega$ and $c = c_1$ on $\mathcal{D} \setminus \Omega$.
- $c = c_0\chi_\Omega + c_1\chi_{\mathcal{D}\setminus\Omega}$ and $c_0, c_1 : \mathcal{D} \to \mathbb{R}$ are Lipschitz functions.
- $\chi_\Omega(x) = 1$ for $x \in \Omega$ and $\chi_\Omega(x) = 0$ for $x \in \mathcal{D} \setminus \Omega$.
- the unknown interface is the boundary of $\Omega$

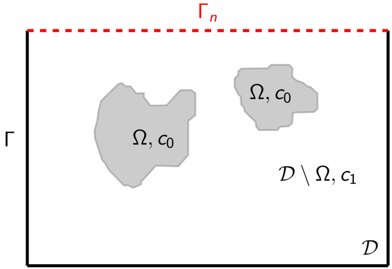


Figure: Piecewise continuous wave velocity $c = c_0\chi_\Omega + c_1\chi_{\mathcal{D}\setminus\Omega}$

# Shape optimization approach for FWI

- Shape optimization approach:

$$\text{minimize} \quad J(\Omega) = \frac{1}{2} \sum_{i=1}^{N_s} \sum_{j=1}^{N_m} \int_0^T (u_i(x_j, t) - d_i(x_j, t))^2 \, dt,$$

- $c = c_0 \chi_\Omega + c_1 \chi_{\mathcal{D} \setminus \Omega}$ is piecewise continuous and the minimization variable is the geometry $\Omega$.
- $\{f_i\}_{i=1}^{N_s}$ is a given set of sources (shots).
- $u_i$ is the acoustic pressure corresponding to $f_i$, $u_i$ depends on $\Omega$ through $c$.
- $d_i(x_j, \cdot)$ denotes the seismogram corresponding to the source $f_i$ and the receiver at $x_j$.
- $c_0$ and $c_1$ can be given or unknown functions, depending on the application.

# Sharp-interface models for salt geometry inversion

- Tikhonov regularization tends to produce smooth velocity models, which precludes the reconstruction of singular features such as sharp interfaces, discontinuities, and high contrasts that are relevant for hydrocarbon exploration.
- An accurate representation of the salt body interface may considerably improve the quality of the images.
- The incorporation of prior information about sharp interfaces and high contrast explicitly in the modeling of the problem is especially advantageous for inverse problems.
- Regularization effect of the sharp-interface assumption.

# Finite elements or finite differences?

- Traditionally, FWI is solved using finite difference methods (FDM) with structured grids.
- The sharp interface of the salt body is irregular in shape and therefore requires relatively fine structured grid resolution to accurately resolve using FDM.
- Finite element methods (FEM) permit the usage of variable unstructured meshes that can more efficiently model these sharp interfaces.
- We rely on a distributed expression of the shape derivative which is more accurate than a boundary expression using FEM.

# Shape derivative

- $T_t : \mathcal{D} \to \mathcal{D}$ is a given diffeomorphism, with $\Omega_t := T_t(\Omega) \subset \mathcal{D}$.
- $J(\Omega_t)$ is a shape functional.
- Shape derivative: $dJ(\Omega)(\theta) = \lim_{t \searrow 0} \frac{J(\Omega_t) - J(\Omega)}{t}$
- Velocity $\theta = \partial_t T_t|_{t=0}$
- Example: $T_t(x) = (I + t\theta)(x)$ for $t \in [0, \tau]$.

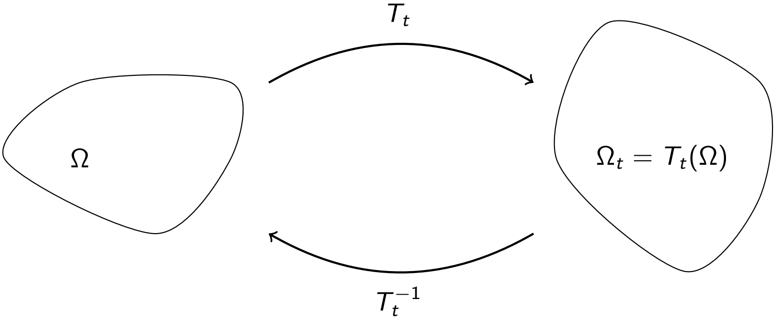

# Adjoint state equation

- Optimize-then-discretize approach (the adjoint state is computed in the continuous domain).
  - The adjoint for the modified acoustic wave equation is given by:

$$
\begin{aligned}
\partial_{tt}^2 u^\dagger - \operatorname{tr}\Psi_1 \partial_t u^\dagger + \operatorname{tr}\Psi_2 u^\dagger - \nabla\cdot(c^2\nabla u^\dagger) - \nabla\cdot(c^2\Psi_2 \boldsymbol{p}^\dagger) & \\
= -\sum_{j=1}^{N_m}[u(x_j) - d(x_j)] & \text{ in } \mathcal{D}\times[0,T], \\
-\partial_t \boldsymbol{p}^\dagger + \Psi_1 \boldsymbol{p}^\dagger + \nabla u^\dagger &= 0 \text{ in } \mathcal{D}\times[0,T], \\
u^\dagger\big|_{t=T} &= 0 \text{ in } \mathcal{D}, \\
\partial_t u^\dagger\big|_{t=T} &= 0 \text{ in } \mathcal{D}, \\
\boldsymbol{p}^\dagger\big|_{t=T} &= \mathbf{0} \text{ in } \mathcal{D}, \\
-\partial_t u^\dagger + c\Psi_2 \boldsymbol{p}^\dagger\cdot\boldsymbol{n} + c\nabla u^\dagger\cdot \mathrm{n} &= 0 \text{ on } \Gamma\times[0,T] \\
\boldsymbol{p}^\dagger\cdot\boldsymbol{n} &= 0 \text{ on } \Gamma\times[0,T]
\end{aligned}
$$

# Shape derivative for FWI

- Cost functional for FWI:

$$J(\Omega) = \frac{1}{2}\sum_{i=1}^{N_s}\sum_{j=1}^{N_m}\int_0^T (u_i(x_j,t) - d_i(x_j,t))^2\,dt.$$

- $d_i$ are the seismograms and $x_j$ the receiver positions.
- Distributed shape derivative in tensor form given by:

$$dJ(\Omega)(\boldsymbol{\theta}) = \int_{\mathcal{D}} \boldsymbol{S}_1 : D\boldsymbol{\theta} + \boldsymbol{S}_0 \cdot \boldsymbol{\theta},$$

$$\boldsymbol{S}_1 = \int_0^T \left[-\partial_t u \partial_t u^\dagger + c^2 \nabla u \cdot \nabla u^\dagger\right] I_n - c^2(\nabla u \otimes \nabla u^\dagger + \nabla u^\dagger \otimes \nabla u)\,dt,$$

$$\boldsymbol{S}_0 = \int_0^T (2c\nabla u \cdot \nabla u^\dagger)\widetilde{\nabla} c.$$

- $\widetilde{\nabla} c(x) := \nabla c_0(x)\chi_\Omega(x) + \nabla c_1(x)\chi_{\mathcal{D}\setminus\Omega}(x) \neq \nabla c(x).$

# Shape morphing

- Shape is represented with an indicator function: $q : \mathcal{D} \times [0, s_0] \to \mathbb{R}$
  - The indicator function $q$ returns a value of 1 for points inside the salt body and 0 elsewhere.
- Model updates/shape morphs are then applied by solving the transport equation to advect this indicator function $q$ for a fixed number of pseudo-timesteps ($\mathcal{O}(10)$):

$$\partial_s q + \boldsymbol{\theta} \cdot \nabla q = 0 \text{ in } \mathcal{D} \times [0, s_0], \tag{0.1}$$

  in which $\boldsymbol{\theta}$ is the descent direction
- We note that (0.1) was solved for 10 pseudo-timesteps, which was a value selected through trial and error. Equation (0.1) was discretized in space using a $0^{th}$ order discontinuous Galerkin (DG0) approach and a $4^{th}$ order Runga-Kutta scheme was used to discretize in time.

# Implementation

- Built using spyro: Acoustic wave modeling in Firedrake
  - https://github.com/krober10nd/spyro
  - Functions to compute descent direction and advect the indicator function $\theta$
- In space:
  - For wave eq.: higher-order mass lumped elements ($P < 5$).
  - For transport eq.: $0^{th}$ order discontinuous Galerkin.
- In time:
  - For wave equation: central finite difference.
  - For transport equation: RK4.

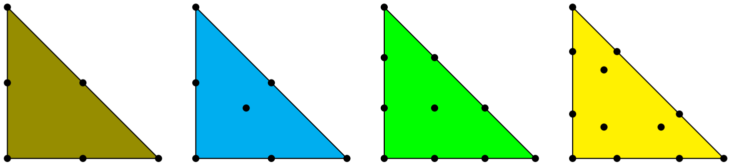

(a) $P_2$ (b) $KMV_2$ (c) $P_3$ (d) $KMV_3$

Figure: Some two-dimensional Lagrange and KMV elements

# Implementation

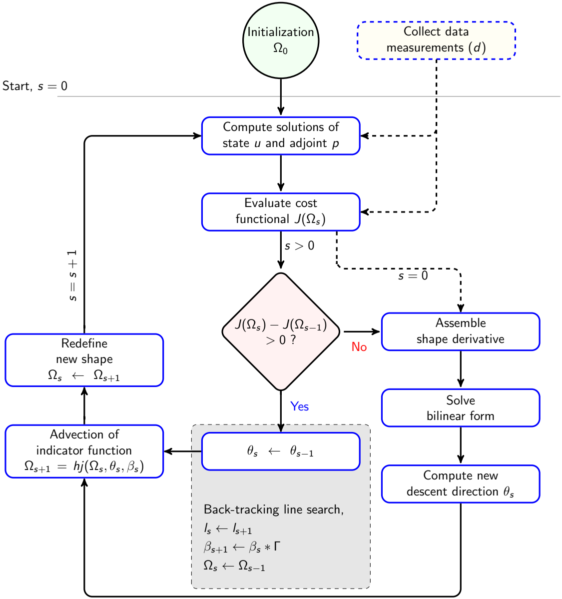

# Unstructured triangular meshes

- Variable resolution, graded triangular meshes adapted to P-wave field.
  - Developed with SeismicMesh: `https://github.com/krober10nd/SeismicMesh`.

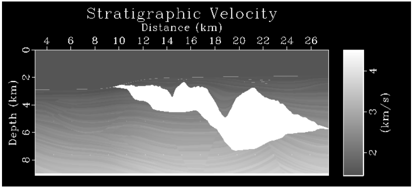


(a) A Sigsbee2b stratigraphy model

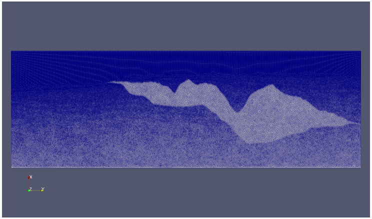

(b) the model meshed with SeismicMesh

Figure: Example of meshing the Sigsbee2b stratigraphy model.

# Numerical results- EAGE Salt

- First we test our implementation with a 2D slice of the EAGE model.
- 20 shots, 3 seconds, 2 Hz noiseless Ricker wavelet

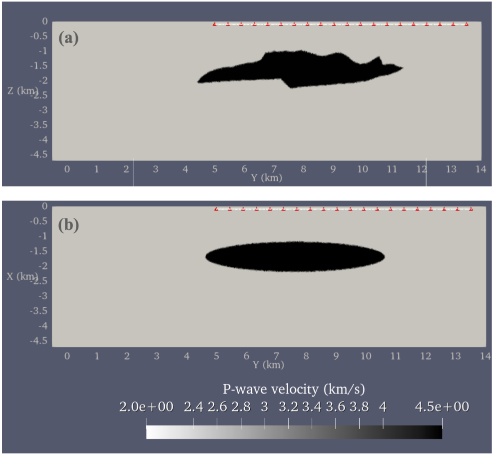


Figure: (a) Target model, (b) starting model. A slice of the EAGE Salt model simplified to two velocities. Sources and receivers are shown in (a),(b).

- After 5 hours and 83 iterations on 20 cores.
- Cost functional exhibited a three order of magnitude reduction from $1.53e-05$ at the first iteration to $7.05e-08$ at the final iteration

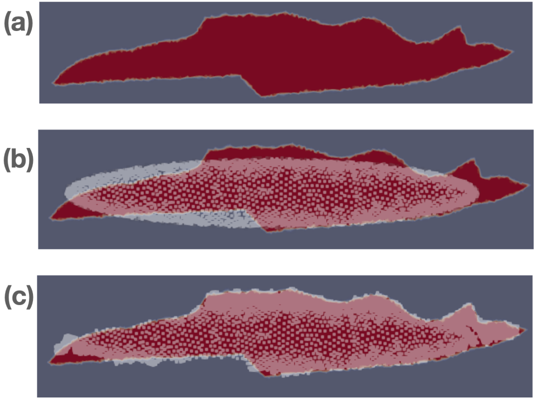


Figure: The optimization results from the EAGE problem.

# Numerical results-Sigbsee2b stratigraphy

- The major difference in this case is the background velocity is non-constant.
- 120 shots, 1000 receivers, 2 Hz noiseless Ricker integrated for 7 seconds.

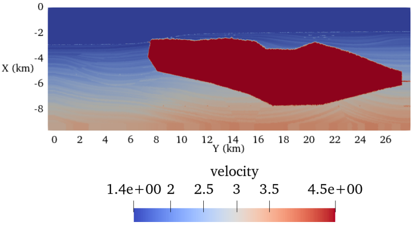


(a) The guess model.

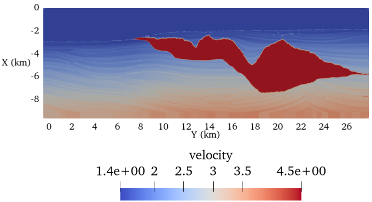


(b) The target model.

Figure: The Sigsbee2b stratigraphy problem.

- The ground truth simulations are conducted on the mesh of the target model and the inversion uses the mesh of the guess model.

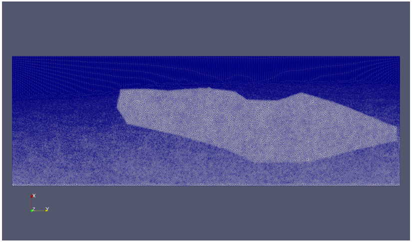

(a) The mesh of the guess model.

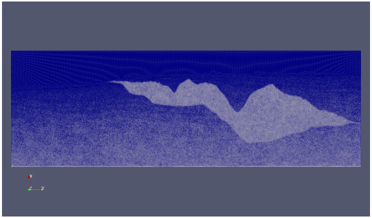

(b) The mesh of the target model.

Figure: Meshes of the Sigsbee2b stratigraphy model.

# Numerical results-Sigbsee2b stratigraphy

- 120 cores (one core per shot) to perform 96 iterations took 13 hours.
- Good agreement along the top of the salt body, little to no change on the bottom-of-the-salt.

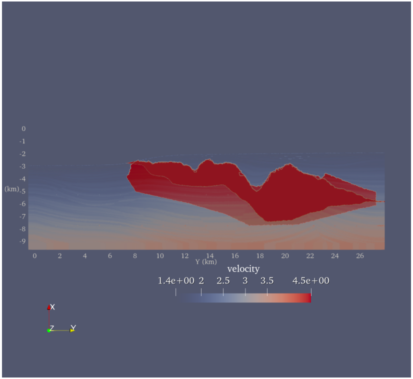


Figure: The final optimization result overlaid on the true velocity model.

# The background velocity $\tilde{c}$

- How to choose this field if it is not known a priori?
  - Special care must be taken so that sharp discontinues don't appear near the salt body's interface with the background velocity field.
  - The background velocity field is fixed throughout the optimization.

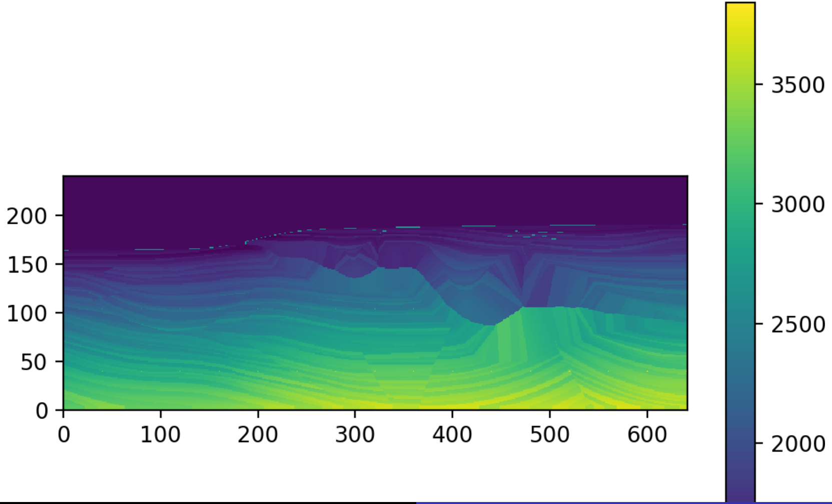

# Numerical results-Sigbsee2b stratigraphy

- Perhaps the optimization region can be targeted with a clever usage of weights.
  - One can see the descent direction is non-zero even on the bottom of the salt.

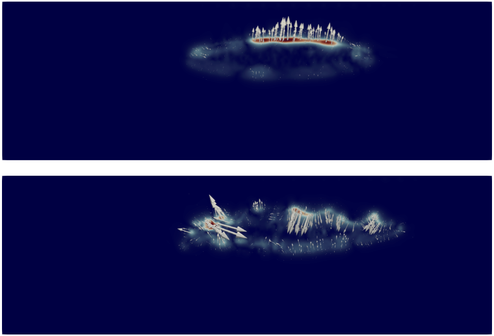

Figure: The descent direction (a) at the first iteration and (b) at the final iteration.